Exploring the ocean microbiome: quantified cobalamin production in pelagic bacteria using liquid chromatography and mass spectrometry

Regina M. Lionheart [1]

regina16@uw.edu

[1] University of Washington, School of Oceanography, Box 357940, Seattle, Washington, 98195-7940

May 11th, 2017

Acknowledgements

First and foremost, I would like to thank my mentor Katherine R. Heal, who helped me through every step of this project. Her patience and expertise were crucial to the production of this research.

I also thank Anitra Ingalls, Arthur Nowell, Julian Sachs, and the School of Oceanography at the University of Washington for funding and supporting the oceanographic sciences.

Abstract

Cobalamin, also known as Vitamin B_{12}, is an essential part of life. It plays a crucial role in the ocean, regulating the metabolic activities of oceanic microbes, which in turn play dynamic roles in carbon cycles and subsequent atmospheric regulation. This research quantifies cobalamin production in two species of bacteria under high and low carbon environments, and in environments enriched with two compounds that may originate from other microbial community members and indicate cobalamin stress. Using liquid chromatography and mass spectrometry, this research shows that for most bioavailable cobalamin, both *R. pomeroyi DSS-3* and *Sulfitobacter sp. SA11* produce more but statistically insignificant cobalamin molecules per cell when grown in high carbon environments, as opposed to when grown in carbon starved conditions. When bacteria were grown in enriched environments, overall cobalamin production was unaffected by stress signaling compounds, although adenosylcobalamin showed significant change in production. Overall, the figures were statistically inconclusive due to small sample size and high intra-sample variation. However, these findings lay groundwork for further research. An important symbiosis involving cobalamin between primary producers and subsections of bacteria and archaea has recently been the subject of metabolomics and proteomics research. The results from this paper provide valuable data for more analysis in this area, by supplying precedent for growing organisms in diluted Seawater Tryptone, and quantitative values of cobalamin production in normal conditions for use in cobalamin models. The findings of this paper highlight both the importance of cobalamin in the ocean microbiome, and the complexity of the microbial interactions in the ocean.

Experimental Workflow

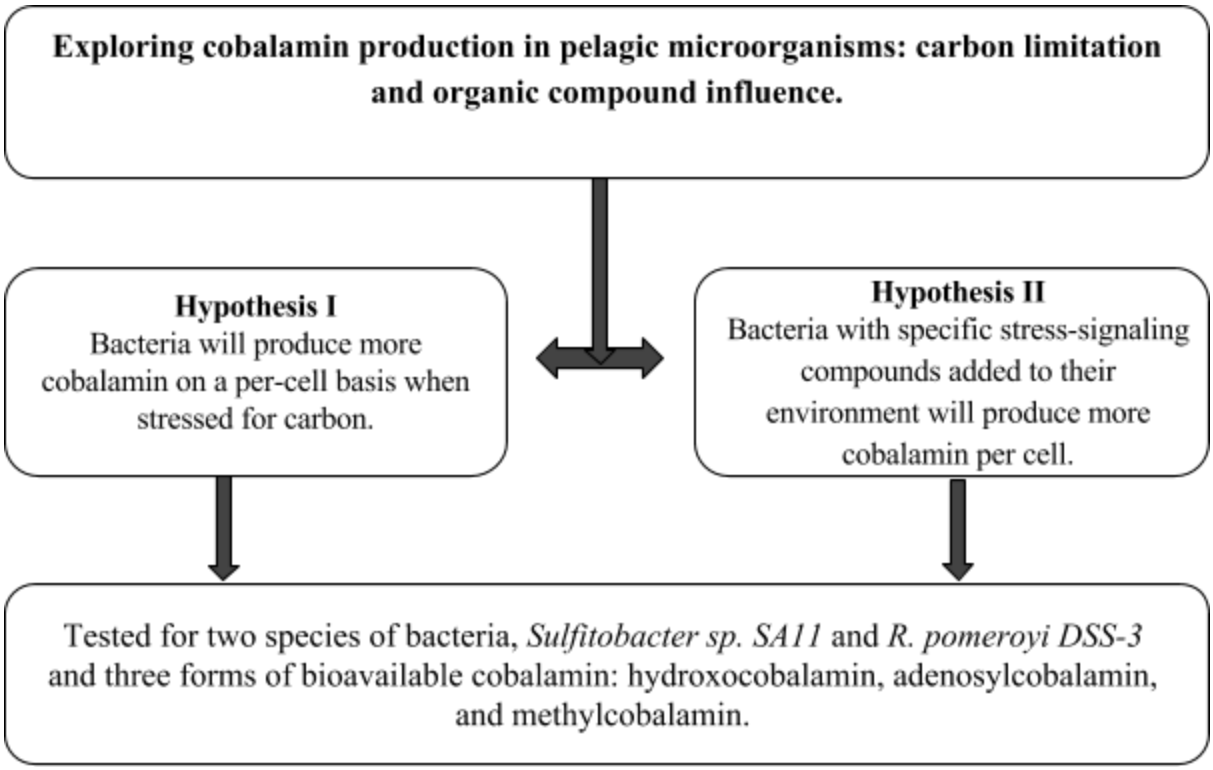

Introduction

Phytoplankton are responsible for half of Earth's primary productivity, and therefore half of atmospheric oxygen. Understanding this microscopic community is imperative, particularly in light of increased emissions of greenhouse gases over the past two centuries. Primary producers do not act independently in the ocean; they sustain relationships with thousands of other organisms in ways that are only recently being recognized and appreciated. Symbiosis, the mutually advantageous relationship between physically associated organisms, is critical to the survival of the oceanic microbiome, and specific compound-based molecular interactions between marine microorganisms have been the subject of much recent research (Amin et al. 2012, Cooper et al. 2015, Ramanan et al. 2015, Johnson et al. 2015). Further understanding of microbiome interconnectivity could illuminate many compelling questions: the evolution of eukaryotic multicellular life (Cooper et al. 2015), influences of primary producers on climate through carbon fixation (Field et al. 1998), and quorum sensing in microbial communities (Johnson et al. 2015) to name a few. Additionally, research into applications of algae for biofuel and nutrient removal in petroleum processing is gaining momentum (Ramanan et al. 2015). Comprehension of the symbiotic biochemical associations within the microbial community is essential to both academia and biotechnology.

Cobalamin auxotrophy (the inability of an organism to synthesize a specific compound necessary for its own growth) is extensive among marine eukaryotic phytoplankton (Croft et al. 2005). However, cobalamin is an essential component of life, and several studies have proven it to be limiting to biomass alone or in conjunction with other nutrients (Koch et al. 2011, Sañudo-Wilhelmy et al. 2014). It comes in several forms, with β ligands consisting of OH-, Ado-, Me-, or CN-. All forms are bioavailable to consumers, but cyanocobalamin is generally not detected in environmental samples. A pressing question is the role that cobalamin has in the life cycles of these oceanic primary producers. It is required for the

metabolic processes of every cell in the human body, yet no eukaryotes possess the biosynthetic pathways for production (Warren et al. 2002). The environmental source in pelagic microbial communities has remained a mystery for many years, though the compound can be biosynthesized by select bacteria and archaea (Sañudo-Wilhelmy et al. 2014). Additionally, there are very few measurements of bioavailable cobalamin free in the environment, insufficient for use by primary producers (Menzel 1962, Carlucci 1970, Sañudo-Wilhelmy et al. 2012). Select bacteria or archaea are considered to be the source of cobalamin utilized by auxotrophic autotrophs, and the ability to accurately measure these released signalling compounds is a recent development (Sañudo-Wilhelmy et al. 2012, Heal et al. 2014, Boysen et al. 2016, Heal et al 2016).

Cobalamin is the most structurally complex of the B vitamins, containing the rare trace metal cobalt and requiring over 20 specific enzymes for biosynthesis. Recent research has suggested a symbiosis between bacteria and eukaryotic autotrophs involving cobalamin and fixed carbon (Koch et al. 2011, Grant et al. 2014, Croft et al. 2015, Lee et al. 2015). It is currently unknown whether this symbiosis between bacteria and eukaryotic algae is passive or active; cobalamin production is metabolically intensive and the symbiosis must be worth the energy required of the heterotrophs to produce it. The levels of cobalamin produced by bacteria in high and low carbon environments are not yet defined, leaving an open question regarding a possible relationship based on fixed carbon and cobalamin production.

This research investigates the cobalamin production on a per cell basis of two species of marine bacteria, *Ruegeria pomeroyi DSS-3* and *Sulfitobacter sp. SA11*, and two organic compounds associated with increased cobalamin output by cobalamin consumers, S-adenosylmethionine (SAM) and S-adenosylhomocysteine (SAH). In a model diatom *T. pseudonana*, SAM levels increase in replete cobalamin conditions, and in depleted cobalamin conditions SAH levels increase (Bertrand et al. 2012, Heal et al. 2016, Heal unpublished). Both species of bacteria have been previously cultured, and their

genomes sequenced (Moran et al. 2007, Amin et al. 2015), making these organisms ideal for laboratory work. The two compounds of interest (SAH and SAM) may relate to increased levels of cobalamin production by bacteria and archaea when incorporating the Croft et al. 2005 symbiosis theory, due to the relationship between cobalamin levels and subsequent production of the compounds by diatoms. Lastly, *SA11* and *DSS-3* are known producers of cobalamin and reliably produce detectable amounts under laboratory conditions (Durham et al. 2015, Heal et al. 2016).

My research investigated two questions that will expand on the current knowledge of the cobalamin production by these organisms. I hypothesize that cobalamin producers control cobalamin output depending on their environment: specifically, carbon-stressed *DSS-3* and *SA11* will release higher levels of cobalamin than those bacteria growing in non carbon-stressed conditions by prioritizing carbon use for cobalamin (Hypothesis I). This supported existing research that defines a interdependence between the bacteria and algae; by producing more cobalamin, bacteria signal to primary producers that the bacteria are in need of the fixed carbon provided by heterotrophs.

The second part of the research investigated the hypothesis that growing bacteria in an environment with added S-adenosylmethionine (SAM), and in another environment with added S-adenosylhomocysteine (SAH), would both result in higher output of cobalamin molecules on a per cell basis by *SA11* and *DSS-3* in both enriched environments (Hypothesis II). SAM is the immediate metabolite of methionine, and the methyl donor for many methylation reactions. Through these reactions, SAM is converted to SAH, and varying ratios of these compounds can signal a cobalamin deficiency in organisms (Guerra-Shinohara et. al. 2004). It has also recently been shown that higher SAM levels are seen in cobalamin-stressed *T. pseudonana* (Heal et al. 2016). The presence of these compounds in the growth environment may signal to bacteria to produce more cobalamin, to maintain symbiosis with the "stressed" primary producers responsible for the compounds. These answers to these questions provide a valuable, quantified link in a global symbiosis.

Methods

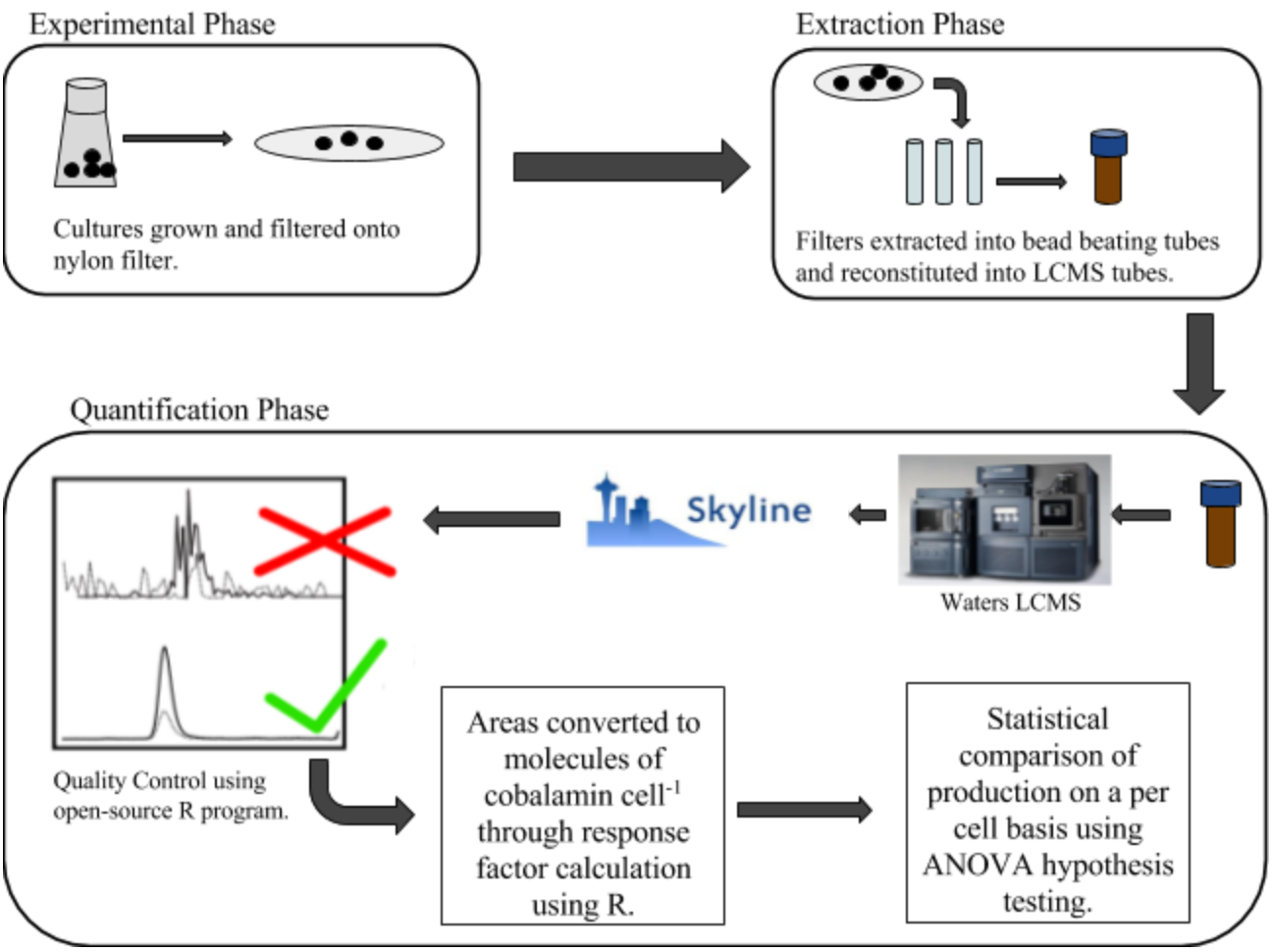

Fig 1. Methods flowchart showing three stages of experiment.

Experimental Phase

Sulfitobacter sp. SA11 and *Ruegeria pomeroyi* DSS-3 were separately cultured for ~24 and ~28 hours respectively (*SA11*, Fig 2. *DSS-3*, Fig 3) in full-strength seawater-tryptone (SWT) broth (30 g Instant Ocean salts, 5 g tryptone in 1 L MQ water) and 1:4 SWT:Instant Ocean artificial seawater. Axenic strains were grown on marine agar petri dishe, picked from freezer stocks kept at -80ºC with 15% glycerol media to prevent freezing. Individual colonies were picked from the plates using sterile loops and inoculated into 3 mL of the respective SWT medias in combusted 15 mL borosilicate culture tubes. They

were shaken at 250 rpm in the dark for 12 hours at 32ºC on a Thermo Scientific Compact Digital Mini Rotator shaker table. Each respective media was inoculated with 500 µL of starter culture into 25 ml of media, with each condition running in triplicate. The flasks were set to shaking at 175 rpm and 32ºC. Cultures were harvested at four time points using a sterile vacuum-powered filtration apparatus, and collected on 0.2 µm Nylon membrane filters (Millipore Co.). After harvesting, the filters were saved in combusted aluminum foil and immediately placed in a -80ºC freezer.

For the experimental phase of the second hypothesis, 50 µL each of 100 mM SAM- and 100 nM SAH-enriched Seawater Tryptone (SWT) were each added to 5 mL of unmodified SWT to make 100 nM enriched media for bacterial growth. Using the same axenic growth techniques described in the first phase of the experiment, *Sulfitobacter sp. SA11* and *Ruegeria pomeroyi DSS-3* were separately cultured in SAM-enriched SWT and SAH-enriched SWT. Both species were also grown in unmodified SWT for comparison of cobalamin production. Using a Beckman Coulter DU 800 spectrophotometer to track growth via optical density at 600 nm, cultures were harvested at exponential growth using the previously described sterile apparatus and filters. Filters were again saved in combusted aluminum foil and placed in a -80ºC freezer.

Extraction Phase

In order to extract metabolites from frozen filters for analysis, a metabolite extraction process was used as described in Rabinowitz 2007 and Heal et al. 2016. In brief, frozen filters from the experimental phase were cut into equal-sized pieces using sterilized tools and equally spread between three MultiPrep FastPrep 2 mL bead-beating tubes. Approximately 1 mL of 50:50 100 µm and 400 µm Ops Diagnostics silica glass beads were added to the tubes for increased mechanical action. A mixture of acetonitrile:methanol:water:formic acid (in 40:40:20 proportions with 0.1% formic acid) was made and stored in a -20ºC freezer, and ~1 mL was added to each bead-beating tube. The tubes were run through a

MultiPrep bead beater three times, resting in the -20ºC freezer for five minutes after each beating round. Tubes were placed in a cooled Eppendorf 5424R microcentrifuge and run at 5000 rpm for 90 seconds. The resulting supernatant was removed with a combusted Pasteur pipette, and placed in a combusted 50 mL glass centrifuge tube. The bead beating tubes with the filters were rinsed once with another ~1 mL of cold 40:40:20 and two times with ~1 mL of cold methanol, each time undergoing bead-beating, centrifugation, and liquid removal to the 50 mL glass centrifuge tube. The tubes were centrifuged in a Beckman Coulter Allegra X-14R Centrifuge and the supernatant removed to combusted 20 mL flat-bottomed tubes and dried down under a stream of clean N_2 air on a ~40ºC heating block. Once dry, the samples were reconstituted in 475 µL LCMS-grade H_2O and 25 µL of an internal standard mixture and filtered through a 0.2 µm teflon filter into a Waters I-Class LCMS vial. The internal standard is an added chemical used for calibration by providing a ratio of analyte signal to internal standard signal.

Quantification Phase

A Waters I-Class Acquity ultra high-pressure liquid chromatography (UPLC) machine coupled with a Waters Xevo triple quadrupole mass spectrometer (TQS) were used to quantify cobalamin in samples by use of standard addition curves. Four standard curves were constructed by running standard additions at the same time as experimental samples, and were analyzed concurrently with samples to quantify cobalamin concentrations under similar LCMS conditions. Consistent 5 µL injections were taken from each vial by the machine for analysis. The raw data from the LCMS returned intensity values for the three types of bioavailable cobalamin tracked in this experiment: methylcobalamin (Me-B_{12}), adenosylcobalamin (Ado-B_{12}), and hydroxocobalamin (OH-B_{12}). Peaks were integrated in Skyline (MacLean et al. 2010) for small molecules, and outputs from Skyline were were run through an open-source R program (Boysen 2016) for quality control and identification of retention time peaks using parameters determined by the Microbial Metabolomics Research Center. Standard curves, which were

prepared at known concentrations to gain a response factor value that could estimate unknown sample concentration values, were returned at expected linear intensity values except for one set (*R. pomeroyi DSS-3* Seawater Tryptone 2). This set encountered injection inconsistency, and missed values were dropped from the linear model to gain a more accurate response factor despite the lower *n* value. The response factors from standard curves were determined through linear models of plotted curves within R, and similarity of concentration curves were checked using coefficient of variation. On both hydroxocobalamin and adenosylcobalamin standard curves, data was processed using best-matched internal standard normalization as described in Boysen et al. 2016 and Heal et al. 2016. Concentration in each sample vial was found from comparative response factors, while cell counts of samples were determined from a conversion factor of optical density data taken during harvesting. Through unit conversions, molecules of cobalamin/cell was obtained from raw area data.

Results

Standard curves were performed in samples that were representative of all sample runs (for example species type, carbon levels, enrichment addition), and the response factor slopes between sample runs within cobalamin types were compared to ensure a low coefficient of variation (CV) between runs (Group comparisons of response factor coefficient of variation are depicted for adenosylcobalamin and hydroxocobalamin in Figs 4 and 5, respectively). Associated linear models and R^2 values for methylcobalamin, hydroxocobalamin, and adenosylcobalamin can be found in the Appendix, Figures 6, 7, 8 respectively. While methylcobalamin showed a raw area CV of 7%, well below the acceptable threshold of ~20%, the adenosylcobalamin response factor CV was 29%, and the hydroxocobalamin CV fell at 93%. In order to mitigate these high levels of variation, a data normalization technique from Heal et al. 2014 was used. Raw analyte area was divided by the matching internal standard area for the internal standards used: B_1, B_2, and B_7. Although normalizing adenosylcobalamin areas to B_2 internal standard areas resulted in an acceptable coefficient of variation of 15% (Fig 4), hydroxocobalamin area modification lowered the CV to only 77% in the case of B_1 internal standard normalization (Fig 5). Despite the high variation, the B_1-modified response factor was used for all subsequent data analysis, and results should be considered with this caveat.

In both species and all environments, methylcobalamin was detected only once within the parameters specified by the Microbial Metabolomics Research Center quality control, in *Sulfitobacter sp. SA11* grown in a high carbon environment (Table 1). Adenosylcobalamin was present in both species under all conditions, with the highest production occurring in *R. pomeroyi DSS-3* under high carbon conditions (Table 1). Hydroxocobalamin molecules per cell showed variable levels in all species and conditions due to detection limits by the LCMS machine, in addition to low signal to noise ratios from low ionization efficiency and high variability in peak quality. The results from the first hypothesis show different levels of adenosylcobalamin produced per cell between high and low carbon conditions in both

species (Table 1). Hypothesis II results regarding adenosylcobalamin production in molecules per cell shows differences in amount produced per cell between enriched media and non-enriched media; there is not a significant difference between the two types of enriched media (Table 2).

Statistical Analysis of Results:

The null hypothesis of Hypothesis I states that cobalamin production per cell will be significantly different as a result of high and low carbon conditions.

Numerically, this is stated as:

$$H_0: \mu_{\text{high carbon}} - \mu_{\text{low carbon}} = 0 \rightarrow \mu_{\text{high carbon}} = \mu_{\text{low carbon}}$$
$$H_a: \mu_{\text{high carbon}} - \mu_{\text{low carbon}} \neq 0 \rightarrow \mu_{\text{high carbon}} \neq \mu_{\text{low carbon}}$$

Whether or not the cobalamin production per cell is significantly different can be determined by t-tests, but many forms of t-tests such as the Student's t-test rely on the assumption that variances between samples are even. In many cases, the variances produced by this experiment are immediately visually dissimilar. This assumption of unequal variances can be confirmed with the two-sample variance-ratio test. The critical F statistic formula is below:

$$F_{obs} = \frac{s_1^2}{s_2^2} \text{ or } F_{obs} = \frac{s_2^2}{s_1^2}$$

The specific F statistic order is determined by whichever sample variance is larger, which always goes in the numerator. From this point, the calculated ratio of sample variances must deviate far enough from 1.0 to reject H_0 at the level of significance, in this case $\alpha = 0.10$. If $F_{obs} < F_{crit}$, do not reject the null hypothesis and assume variances are equal. Once variance equality is determined, either a Student's t-test (for equal variance) or a Welch's t-test (for unequal variance) will be used for equality of average cobalamin production.

All following equations show statistical testing for Hypothesis I in the example of *R. pomeryoi DSS-3* adenosylcobalamin molecules per cell comparison (Table 1). For all subsequent statistical analysis for Hypotheses I and II, data were tested through R and displayed in Tables 3 and 4.

***DSS-3* adenosylcobalamin molecules per cell F-test**

$$F_{obs} = \frac{s^2_{DSS-3,\,Low\ Carbon}}{s^2_{DSS-3,\,High\ Carbon}} = \frac{4628.95}{1117.63} = 4.14$$

$$F_{crit} = F_{0.1(2),\,2,\,2} = 9$$

Because $F_{obs} < F_{crit}$, we do not reject the null hypothesis that variances are equal and continue with a student's t-test.

***DSS-3* adenosylcobalamin molecules per cell student's t-test, assuming equal variances.**

The test statistic for the student's t-test is:

$$t_{obs} = \frac{\left|\bar{x}_1 - \bar{x}_2\right| - \delta}{s_{\bar{x}_1 - \bar{x}_2}}$$

Under the assumption of $\sigma_1^2 = \sigma_2^2$, a pooled estimate of the variance is used.

$$s_{\bar{x}_1 - \bar{x}_2} = \sqrt{s_p^2 \left(\frac{1}{n_1} + \frac{1}{n_2}\right)}, \text{ with } s_p^2 = \frac{(n_1 - 1)s_1^2 + (n_2 - 1)s_2^2}{n_1 + n_2 - 2}$$

Applying this formula to experimental values, we obtain the following *R. pomeroyi DSS-3* molecules of adenosylcobalamin per cell.

Symbol	**Experimental value**
$\bar{x}_{DSS-3,\,High\ Carbon}$	443.94 adenosylcobalamin cell^{-1}
$\bar{x}_{DSS-3,\,Low\ Carbon}$	366.13 adenosylcobalamin cell^{-1}
δ	0 (when testing for equal means)
$s^2_{DSS-3,\,High\ Carbon}$	1117.63
$s^2_{DSS-3,\,Low\ Carbon}$	4628.95

$n_{DSS-3,\ High\ Carbon}$ & $n_{DSS-3,\ Low\ Carbon}$	3

$$s_p^2 = \frac{(3-1) * 1117.63 + (3-1) * 4628.95}{3 + 3 - 2} = 2873.29$$

$$s_{\bar{x}_{DSS-3,\ High\ Carbon} - \bar{x}_{DSS-3,\ Low\ Carbon}} = \sqrt{2873.29\left(\frac{1}{3} + \frac{1}{3}\right)} = 43.77$$

$$t_{obs} = \frac{|443.94 - 366.13| - 0}{43.77} = 1.78$$

We compare the t_{obs} value of 1.78 to the $t_{critical}$ value from a standard t-table, which corresponds to $t_{\alpha(x),\ v} = 2.132$. When $t_{critical} < t_{obs}$, the null hypothesis is rejected and the means are assumed to be statistically different. In this case, $t_{critical} 2.132 > t_{obs} 1.78$, and so we reject the hypothesis that molecules of adenosylcobalamin cell^{-1} produced by *R. pomeryoi DSS-3* under high and low carbon conditions were statistically different in this experiment.

The above statistical tests (F-test followed by appropriate t-test) are repeated for comparison of adenosylcobalamin production per cell between high and low carbon environments in *SA11*, and combined cobalamin production between high and low carbon environments for both organisms. Statistical analysis for the results of Hypothesis I are displayed in Table 3.

DSS-3 adenosylcobalamin molecules per cell ANOVA test

Similar to t-tests, a one way ANOVA test compares differences among means and determines whether those differences are statistically significant or can be attributed to chance. For Hypothesis II, it is more advantageous to use an ANOVA instead of multiple t-tests due to the 2+ study groups in the data (SAM, SAH, and SWT). Using multiple t-tests for three more categories increases the chance of making Type I error (i.e., incorrect rejection of a true null hypothesis). Setting a single $\alpha = 0.1$ for the ANOVA keeps the probability of Type I error at that level for the duration of the analysis.

Similar to the Welch and Student's t-test, the null hypothesis of ANOVA states that the means are equal, $H_0 : \mu_1 = \mu_2 = \mu_3$. The alternate hypothesis states that at least two of the averages are not equal to the others. When run through an ANOVA-F test in R, the following output is produced:

```
             Df Sum Sq Mean Sq F value Pr(>F)
condition    2  10314    5157    5.43 0.0451 *
Residuals    6   5698     950
---
Signif. codes:  0 ‘***’ 0.001 ‘**’ 0.01 ‘*’ 0.05 ‘.’ 0.1 ‘ ’
```

With an F-statistic of 5.43 and a p-value of 0.0451 (<0.1), the null hypothesis is rejected and we can confirm that results are just within the statistically significant bounds of difference between the treatments. Considering the low sample size, this p-value may have been due to chance. To confirm what is driving the difference between treatments, a Tukey's Honestly Significant Differences test (Tukey's HSD) is used to show which treatments were most significant.

```
       diff        lwr       upr     p adj
SAM-SAH   7.683333  -55.62727  70.99393 0.9503173
SWT-SAH -67.660000 -130.97060  -4.34940 0.0802993
SWT-SAM -75.343333 -138.65393 -12.03273 0.0547789
```

The bolded values show that results which are not significantly different: the comparison between molecules of adenosylcobalamin per cell in DSS-3 from environments enriched with SAM and SAH. However, the production of molecules per cell in enriched environments differ significantly from the unenriched SWT environment.

All subsequent significance calculations for the results of Hypothesis II are in Table 4.

Discussion

This research sought to illuminate cobalamin production in two species of marine bacteria under varying conditions, and to quantify this production on a molecule per cell basis using liquid chromatography paired with tandem mass spectrometry. Further understanding of how this metabolically expensive, cobalt-containing molecule cycles through the ocean has implications for many molecule-based interactions between microbes in the epipelagic and mesopelagic zones. This goal was defined in two hypotheses, the first being that two cobalamin producing bacteria, *Sulfitobacter sp. SA11* and *R. pomeroyi DSS-3,* would produce more cobalamin on a per cell basis when grown in an environment with more carbon. This first hypothesis also provides valuable data to build upon for continuing experiments that require microbial growth in diluted solutions. The second hypothesis quantified cobalamin per cell in both species of marine bacteria under environments enriched with important methylating agents, S-adenosylmethionine (SAM) and S-adenosylhomocysteine (SAH). In a well-documented cobalamin exchange symbiosis between diatoms and bacteria (Croft et al. 2005, Koch et al. 2011), it has been shown that cobalamin starvation in diatoms corresponds to lower levels of SAM production, and higher levels of SAH (Heal et al. 2016), as methylcobalamin is a required coenzyme in the synthesis of methionine from homocysteine. Therefore, the presence of SAH, the demethylated derivative of SAM, may signal to bacteria to produce more cobalamin.

This experiment monitored all four forms of cobalamin, but presents the results of the three biologically relevant forms (OH-, Ado-, and Me-). Methylcobalamin was below the level of detection in all samples except for *Sulfitobacter sp. SA11* growing in high carbon conditions (Table 1). As one of the forms of cobalamin that is actively used as a cofactor in methylcobalamin-dependent methyltransferase enzymes and as an unstable form of cobalamin that is highly susceptible to photodegradation to adenosylcobalamin (Banerjee et al 2003, Heal et al 2012), it is possible that the methylcobalamin present in samples simply converted to adenosylcobalamin. Due to the high levels of adenosylcobalamin found in most samples, this is a possible fate of the methylcobalamin.

It is perhaps most valuable to look at the total production of all forms of cobalamin added together for each condition, as all types measured in this experiment are all bioavailable to other microbial community members. For Hypothesis I, the results from these calculations show less conclusive results than isolated cobalamin forms (Table 1). There was no statistical difference between cobalamin per cell in either species, and this is clear from the direct numerical results as well. Changing the carbon did not appear to change the overall amount of cobalamin produced and/or detected. This was echoed in Hypothesis II, where overall cobalamin production was not affected by the addition of SAH or SAM. The combined results echo the isolated results, and indicate the highest production of cobalamin per cell in Hypothesis II is in enriched media for *DSS-3*. This trend is reversed in *SA11* in the same hypothesis. No combined cobalamin results reflect a statistically significant difference between enriched and unenriched medias. However, more information can be gained from looking into the comparison of cobalamin derivatives (Me-B_{12}, Ado-B_{12}, OH-B_{12}).

The results for Hypothesis I suggest there may be a relationship between carbon levels and cobalamin per cell when examining the forms, though it was opposite of our initial hypothesis. Under high carbon conditions,both *SA11* and *DSS-3* produced more adenosylcobalamin (Table 1). This suggests that at least within this form, cobalamin production per cell and carbon level are directly correlated. Hydroxocobalamin showed less conclusive results, particularly in *DSS-3* high carbon (Table 1). In low carbon conditions, the bacteria produced 227 ± 142 molecules of hydroxocobalamin per cell, while in high carbon, the total was 52 ± 27 molecules of hydroxocobalamin per cell. Hydroxocobalamin is a challenging compound to measure: its interaction with the LC column can result in wide chromatogram peaks and low signal to noise ratios. Due to this high intra sample variability, hydroxocobalamin production in *DSS-3* was not statistically significant. The numbers from the results table are drawn from the average of three replicates, and in the case of this sample, two samples produced low signal to noise ratios and did not make it past the R quality control program. However, the overall area of these two

samples were significant, and their results are reflected in the totals in Table 1. Although the numbers of *DSS-3* adenosylcobalamin molecules per cell in high carbon were still lower than those in low carbon, it is present and detected by the machine.

The results from the second hypothesis (Table 2), while showing no significant difference in overall cobalamin production between treatments, do reflect significance in adenosylcobalamin. For adenosylcobalamin, there was an interesting result between *DSS-3* and *SA11*. The production of adenosylcobalamin molecules per cell in *DSS-3* showed a statistically significant difference between enriched and unenriched media using an ANOVA test (Table 4), and further analysis showed that the difference was only present between enriched and unenriched medias as a whole, with no difference between the types of enriched media. Interestingly, the results from *SA11* for the same conditions show precisely the opposite trend, with cells grown in unenriched seawater tryptone producing the most adenosylcobalamin on a per cell basis (Table 1), although these data were not concluded to show statistically significant differences. Further research may show that even relatively closely related organisms may have different adenosylcobalamin responses to varying levels or ratios of SAM and SAH, increasing metabolic diversity within the already vast arrays of metabolic functions.

Hydroxocobalamin results in *DSS-3* under Hypothesis II were significantly different than those from *SA11*, which showed almost no production per cell. Within *DSS-3* results, there was a visual pattern in hydroxocobalamin production that would support Hypothesis II; however, the differences between enriched and unenriched seawater were not statistically significant at a 90% confidence level. *DSS-3* grown in media enhanced with SAH and SAM showed highly variable production, with a standard deviation around ~400 molecules hydroxocobalamin per cell (~60% and ~80%) between replicates in both cases. It is possible that hydroxocobalamin production in this organism with enriched seawater could be could be much higher but was lowered due to variation, and subsequent experiments could clarify. Methylcobalamin was undetected in all samples.

The discrepancy between *SA11* and *DSS-3* in terms of production levels could be due to several factors. Under all conditions and in all forms of cobalamin, *SA11* produced fewer molecules cobalamin per cell than *DSS-3* when detected (Table 1). A model organism for lab culturing since its isolation from coastal Georgia waters in 1998, *DSS-3* has been used in many lab experiments regarding cobalamin production and phytoplankton growth, and readily produces molecules for study (Durham et al. 2015, Johnson et al. 2015, etc). In fact, it actually produces far more cobalamin than it apparently needs for its own metabolic functions, and may be contributing to other unknown microbial relationships. It is often found in coastal blooms and tends to be densely populated in those areas. *Sulfitobacter sp. SA11* is a smaller, recent isolate, cultured from Puget Sound in 2015 (Amin et al. 2015), and may be a less productive source of cobalamin. Additionally, the conversion factor used for transforming optical density data to cell count for *SA11* may not be fully linear, and may not accurately scale down to very small numbers. However, an encouraging note is a recent study by Heal et al. 2016 that shows very similar numbers of cobalamin molecules per cell in both organisms. This is a good indicator that the methods used for quantifying cobalamin production are robust. During the experimental phase of the research, *DSS-3* was harvested towards the end of its growth curve (Fig 2), and *SA11* were harvested during or just before exponential growth. Although data was normalized to account for optical density, this may contribute to the highly variable levels of hydroxocobalamin and adenosylcobalamin between organisms.

In conclusion, these experiments give valuable insight into quantified cobalamin production within the ocean microbiome. These data lay the groundwork for further development of the hypotheses, such as testing the effect on cobalamin production of both marine bacteria co-cultured with a cobalamin-stressed diatom (e.g the model diatom *Thalassiosira pseudonana*) to investigate untargeted signalling molecules in filtrate. Understanding more of the ratio of cobalamin types within organisms may have indications for the efficiency or health of the organism. However, the research completed thus far suggests that the symbiosis between bacteria and some primary producers (Croft et al. 2005) could be

linked to the specific molecules of S-adenosylmethionine and its demethylated derivative, S-adenosylhomocysteine. Additionally, although the plasticity of cobalamin production by heterotrophs is still unclear, this research suggests that cobalamin production is fairly consistent over highly variable growth conditions, which is vital for cobalamin production models. Further research will illuminate more details of this symbiosis and microbial interdependencies, and give insight into how the marine microbiome is shaped through its chemical interactions.

References

Amin, S.A., M.S. Parker, E.V. Armbrust. 2012. Interactions between diatoms and bacteria. Microbiology and Molecular Biology Reviews: **76** (3): 667 - 684

Amin, S.A., L.R. Hmelo, H. M. van Tol, B.P. Durham, L.T. Carlson, K.R. Heal, R. L. Morales, C.T. Berthiaume, M.S. Parker, B. Djunaedi, A. E. Ingalls, M. R. Parsek, M. A. Moran, E. V. Armbrust. 2015. Interaction and signalling between a cosmopolitan phytoplankton and associated bacteria. Nature Letter.

Bannerjee, R. S.W. Ragsdale. 2003. The many faces of vitamin B_{12}: catalysis by cobalamin-dependent enzymes. Annual Review of Biochemistry **72**: 209 - 247

Bertrand, E.M., A.E. Allen, C.L. Dupont, T.M Norden-Krichmar, J. Bai, R.E. Valas, M.A. Saito. 2012. Influence of cobalamin scarcity on diatom molecular physiology and identification of a cobalamin acquisition protein. Proceedings of the National Academy of Science **109** (26): 1762 - 1771

Boysen, A.K. October 2016. Ingalls Lab UW Quality Control. Source code. https://github.com/IngallsLabUW/QualityControl.

Boysen, A.K., K. R. Heal, L. T. Carlson, A. E. Ingalls. 2016. A paired hydrophilic interaction and reverse phase chromatography method for targeted metabolomics of environmental samples addressing sample specific matrix effects. Submitted to Analytical Chemistry Nov. 2016.

Carlucci, A.F. 1970. The ecology of the plankton off La Jolla, California in the period of April through September, 1967. Bulletin of the Scripps Institution of Oceanography **17**: 23 - 33

Cooper, M. B and A.G. Smith. 2015. Exploring mutualistic interactions between microalgae and bacteria in the omics age. ScienceDirect **26**: 147 - 153

Croft, M. T., A.D. Lawrence, E. Raux-Deery, M.J. Warren, A.G. Smith. 2005. Algae acquire vitamin B_{12} through a symbiotic relationship with bacteria. Nature **438**: 90 - 93

Durham, B. P., S. Sharma, H. Luo, C. B. Smith, S. A. Amin, S. J. Bender, S. P. Dearth, B. Van Mooy, S. R. Campagna, E. B. Kujawinski, E. V. Armbrust, M. A. Moran. 2015. Cryptic carbon and sulfur cycling between surface ocean plankton. Proceedings of the National Academy of Science **112** (2): 453 - 457

Falkowski, P.G. 1993. The role of phytoplankton photosynthesis in global biogeochemical cycles. Photosynthesis Research **39**: 235 - 258

Field, C.B., M.J. Behrenfield, J.T. Randerson, P. Falkowski. 1998. Primary production of the biosphere: integrating terrestrial and oceanic components. Science **5374** (281): 237 - 240

Grant, M. A., E. Kazamia, P. Cicuta, A.G. Smith. 2014. Direct exchange of vitamin B_{12} is demonstrated by modelling the growth dynamics of algal-bacterial cultures. The ISME Journal 1 - 10

Guerra-Shinohara, E.M, O.E Moria, S. Peres, R.A Pagliusi, L.F Sampaio, V. D'Almeida, S.P. Irazusta, R.H. Allen, S.P. Stabler. 2004. Low ratio of S-adenosylmethionine to S-adenosylhomocysteine is associated with vitamin deficiency in Brazilian pregnant women and newborns. PubMed.gov.

Heal, K.R., L.T. Carlson, A. H. Devol, E. V. Armbrust, J.W. Moffett, D. A. Stahl, A. E. Ingalls. 2014. Determination of four forms of vitamin B12 and other B vitamins in seawater by liquid chromatography/tandem mass spectrometry. Rapid Communications in Mass Spectrometry **28** (22): 2398 - 2404

Heal, K.R., W. Qin, F. Ribalet, A.D. Bertagnolli, W. Coyote-Maestes, L.R. Hmelo, J.W. Moffett, A.H. Devol, E.V. Armbrust, D.A. Stahl, A.E. Ingalls. 2016. Production and demand of two distinct pools of B_{12} analogs reveal unexpected community interdependencies in the ocean. Proceedings of the National Academy of Science.

Johnson, W. M., M. C. Koule, E. B. Kujawinski. 2015. Evidence for quorum sensing and differential metabolite production by a marine bacterium in response to DMSP. The ISME Journal 1 - 13

Koch, F., M. A. Marcoval, C. Panzeca, K.W. Bruland, S. A. Sañudo-Wilhelmy, C. J. Gobler. 2011. The effect of vitamin B_{12} on phytoplankton growth and community structure in the Gulf of Alaska. Limnology and Oceanography **56** (3): 1023 - 1034

Lee, P. A., E. M. Bertrand, M. A. Saito, G. R. DiTullio. 2015. Influence on vitamin B_{12} availability on oceanic dimethylsulfide and dimethylsulfoniopropionate. Environmental Chemistry **13** (2): 293 - 301

MacLean, B., D.M. Tomazela, N. Shulman, M. Chambers, G.L. Finney, B. Frewen, R. Kern, D.L. Tabb, D.C. Liebler, M.J. MacCoss. 2010. Bioinformatics **26**: 966– 968

Menzel, D.W., J.P. Spaeth. 1962. Occurrence of vitamin B_{12} in the Sargasso Sea. Limnology and Oceanography **7** (2): 151 - 154

Moran, M.A., R. Belas, M.A. Schell, J.M. González, F. Sun, S. Sun, B. J. Binder, J. Edmonds, W. Ye, B. Orcutt, and ten others. 2007. Ecological Genomics of Marine Roseobacters. Applied and Environmental Microbiology **73** (14): 4559 - 4569

Rabinowitz, J.D., E. Kimball. 2007. Acidic acetonitrile for cellular metabolome extraction from Escherichia coli. Analytical Chemistry **79** (16): 6167–6173

Ramanan, R., B. Kim, D. Cho, H. Oh, H. Kim. 2015. Algae-bacteria interactions: Evolution, ecology and emerging applications. Biotechnology Advances **34**: 14 - 29

Sañudo-Wilhelmy, S.A., L.S. Cutter, R. Durazo, E.A. Smail, L. Gómez-Consarnau, E.A. Webb, M.G. Prokopenko, W.M. Berelson, D.M. Karl. 2012. Multiple B-vitamin depletion in large areas of the coastal ocean. Proceedings of the National Academy of Science **109** (35): 14041–14045

Sañudo-Wilhelmy, S.A., L. Gomez-Consarnau, C. Suffridge, E.A. Webb. 2014. The Role of B vitamins in marine biogeochemistry. Annual Review of Marine Science **6**: 339 - 367

Warren, M. J., E. Raux, H. L. Schubert, J. C. Escalante-Semerena. 2002. The biosynthesis of adenosylcobalamin (vitamin B_{12}). Natural Product Reports **19**: 390 - 412

Appendix

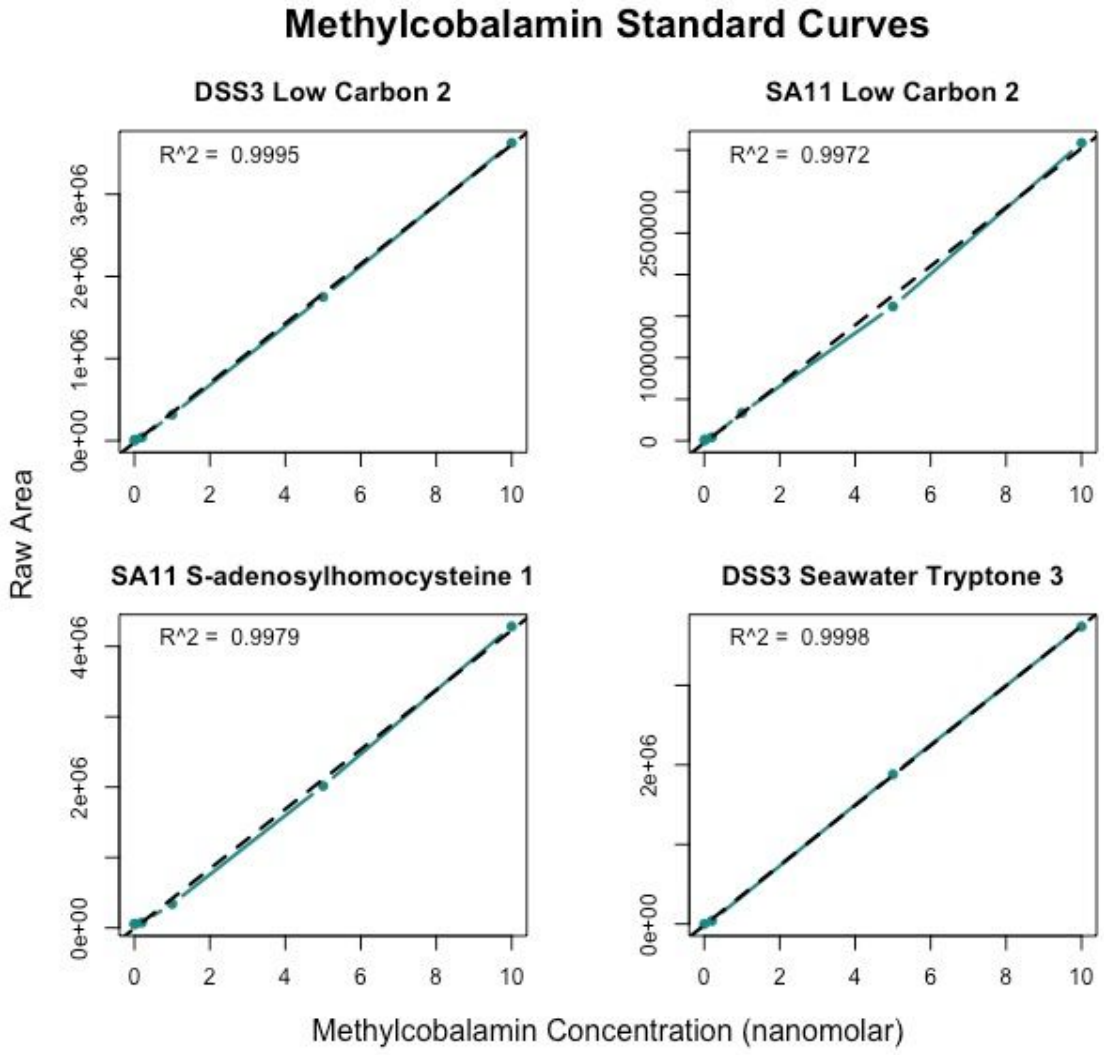

Fig 6. Methylcobalamin standard curves, unmodified by internal standard division.

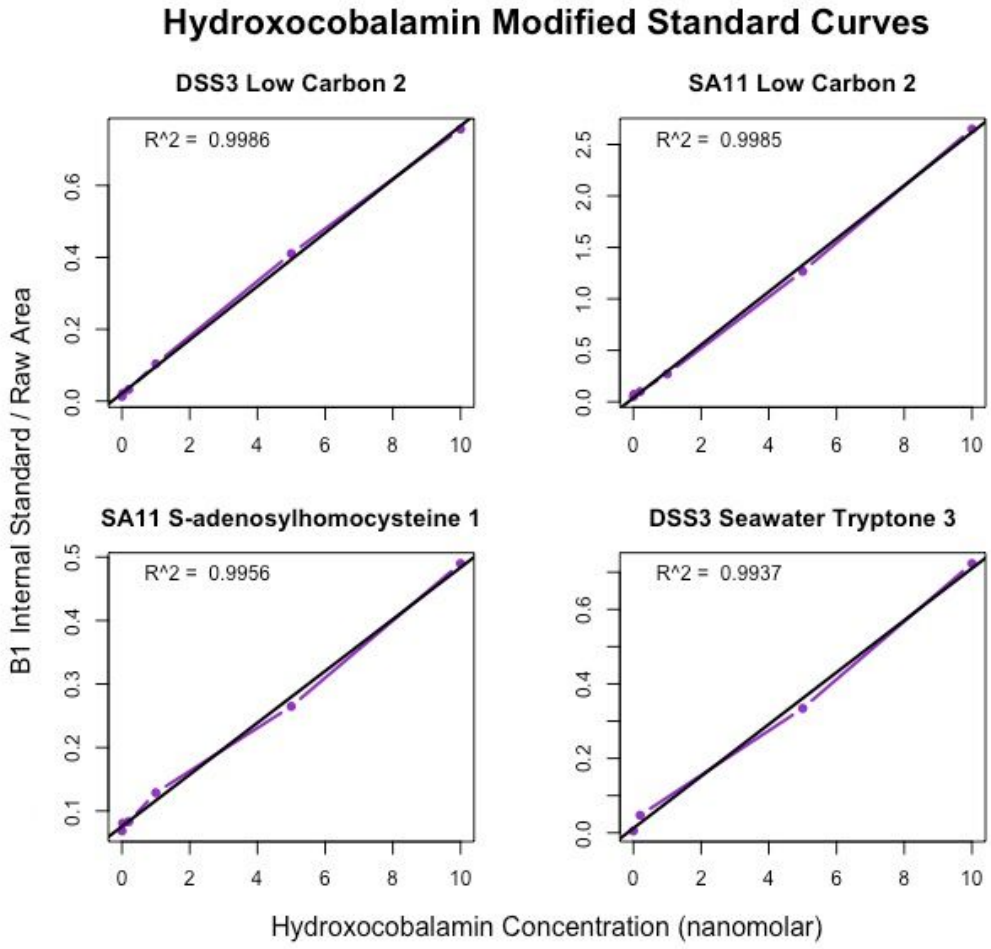

Fig 7. Hydroxocobalamin standard curves, modified by Heal 2016 internal standard normalization process. Vitamin B_1 internal standard produced the lowest coefficient of variation between slopes (Fig 2).

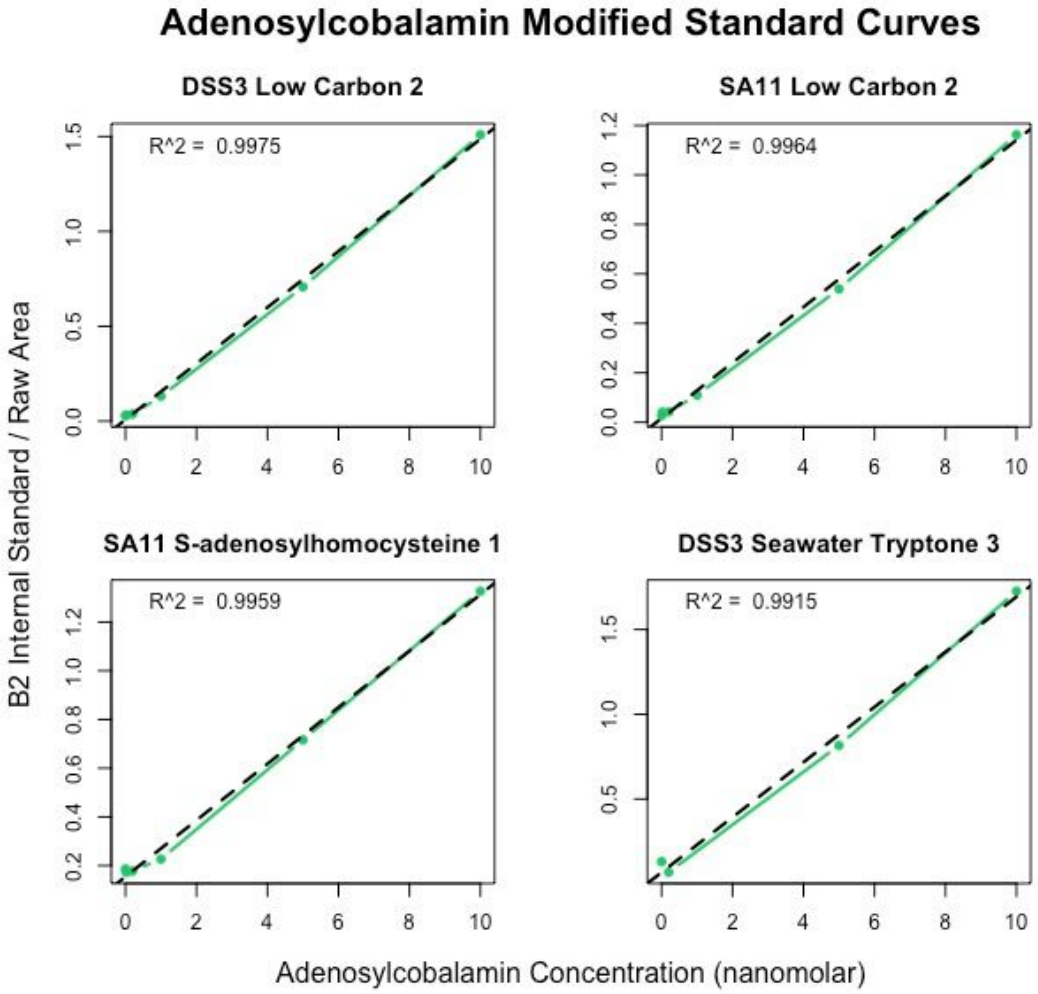

Fig 8. Adenosylcobalamin standard curves, modified using Vitamin B_2 internal standards (Fig 1).